

A Rayleigh lidar study of the atmospheric temperature structure over Mt. Abu, India

H.Chandra, Som Sharma, Y.B.Acharya and A.Jayaraman
Physical Research Laboratory, Navrangpura, Ahmedabad - 380 009
E.mail : hchandra44@gmail.com

ABSTRACT

A Nd-YAG laser based Rayleigh Lidar was set up at Guru Shikhar, Mount Abu (24.5° N, 72.7° E, altitude 1.7 km) by the Physical Research Laboratory to study the temperature structure in the altitude region of 30-75 km at tropical latitudes. Temperature profiles are derived from relative density measurements, following the method described by Hauchecorne & Channin (1980). Photon counts are averaged over one hour (2 hour during the later phase) in time and 480 m in altitude. Measurements were made for about 5 nights of each month around new moon except the monsoon season (June-August). Temperature profiles obtained on 109 nights during the period November 1997 to November 2001 are used to derive average temperature profile for each month (September to May) and are compared with the CIRA-86 model. Observed temperature profiles are in good agreement with CIRA-86 below 50 km but are higher by up to 10 K above 50 km. The agreement is better during winter months. The temperature profiles are also compared with the equatorial model for the Indian region (Sasi & Sengupta 1979) based on rocket and balloon measurements. Day to day variability is less than ± 5 K for altitudes below 50 km and up to ± 10 K around 70 km. The variability is the least around 40-50 km. The mean values of the stratopause level and temperature are found to be 48 km and 271 K respectively over the measurement site. Seasonal variation of the temperature below 60 km shows equinoctial and summer maxima whereas above 70 km winter maximum with equinoctial minima are seen.

INTRODUCTION

Lidar has emerged as a powerful technique for active remote sensing of the middle atmosphere. Lidar probing of the atmosphere utilises both scattering and absorption by the medium (Kent & Wright 1970; Hinkley, 1976; Hauchecorne & Chanin 1980; Clemesha 1984; Thomas, 1987; Gardner, 1989; Menzies & Hardesty, 1989; Browell, 1989; Reagan, McCormick & Spinhirne 1989; and Thomas et al., 1996).

Rayleigh scattering by air molecules has been used extensively to determine the density of the atmosphere in the region of 30 to 90 km (Kent and Wright, 1970; Hauchecorne & Chanin 1980; Chanin & Hauchecorne, 1981, 1984, 1996, Shibata, Kobuchi & Maeda 1986a; Shibata, Fukuda & Maeda 1981 b; Jenkins et al. 1987; Whiteway & Carswell 1994). Temperature profiles are derived from relative density data assuming that the atmosphere obeys the barometric equation. From the perturbations in the density or temperature profiles one can also determine gravity wave features.

Lidar probing of the atmosphere was initiated at the Physical Research Laboratory (PRL) in the early

nineties. A powerful Nd-YAG laser based lidar (operating at 532 nm) with a 40 cm Cassegrain telescope was made operational at Ahmedabad (23.1° N, 72.5° E) in April 1992 and used primarily for aerosol studies (Jayaraman et al. 1995a). The decay of the aerosol layer following the Mt. Pinatubo eruption was studied from the observations that continued till 1995 (Jayaraman et al. 1995b). During 1995 some observations with integration time of one hour were made at Ahmedabad to obtain density measurements from the Rayleigh scattered signals above 30 km. However the measurements could be made up to about 60 km only with a 40-cm aperture telescope (Jayaraman et al. 1996).

The system was moved to a new site at Guru Shikhar (24.5° N, 72.7° E), in Mt. Abu in 1997 where a bigger 90-cm diameter telescope was set up and regular measurements for temperature studies were started. Temperature profiles could be derived up to 70-75 km altitude with an integration time of one to two hours. Regular measurements of density/temperature have been made since November 1997 and the lidar is operated for about 5 nights each month. During the monsoon period, which basically

lasts from mid June to mid September over the site, regular measurements are not possible due to poor weather condition and only a few nights of observations could be made during clear sky condition. A total of 125 nights of observations were made in the Rayleigh mode of operation during the period from November 1997 to November 2001, out of which 109 nights have provided data of sufficient quality to yield temperature profiles. Monthly mean temperature profiles have been obtained in the altitude range from 30 to 75 km for the months September to June. The Rayleigh lidar system used at Mt. Abu and the temperature profiles obtained during this period are described here.

METHODOLOGY

Lidar equation

The lidar equation relates the power received at a particular instant of time to the power transmitted (Hinkley 1976; Measures 1984). For a Rayleigh lidar the number of photons $N_s(z)$ detected at an altitude z can be expressed as

$$N_s(z) = K [\rho_a(z)/(z-z_T)^2] T_a^2(z, z_T) \quad (1)$$

Where, K is a system constant. It depends on the laser power, range and time integration used, collecting area of the telescope, altitude, the optical efficiency of the mirrors, lenses, filters and the quantum efficiency of the photo multiplier tube. Z_T is 1.7 km for the lidar site at Mt. Abu. For the 1 nm band pass filter used in the present set up, the transmission efficiency is about 20 % and the quantum efficiency of the PMT is about 9 % at 532 nm. T_a is the one way transmittance of the lower atmosphere and depends on the wavelength used and the atmospheric turbidity. $\rho_a(z)$ is the atmospheric density (m^{-3}).

Density Measurements

The relative atmospheric density can be derived from equation (1). For Rayleigh lidar the extinction of the laser beam as it propagates in the atmosphere is negligible at altitudes above 30 km. Therefore assuming T_a to be equal to 1, the relative atmospheric density is given by

$$\rho_a(z) = (z-z_T)^2 [N_s(z) - N_b] / K \quad (2)$$

In addition to the photon counts due to the backscattered signal there is background photon count, N_b . This is given by the product of the background noise and the dark counts per range bin per pulse, with the laser pulse rate and the integration time.

Noise term N_b is computed from the photon counts at much higher altitudes (from 85 to 95 km). For absolute density comparison with an independent measurement or with model values, calibration of the system is required. The number of photon counts received is related to the laser power, area of telescope, range bin and integration time. Therefore powerful lidar systems with large telescope area are required for density measurements up to 80 km. The relative error in relative density is proportional to inverse square root of the received photon counts.

Temperature derivation

Temperature profile is derived from relative density profile assuming the atmosphere obeys the barometric equation (Hauchecorne & Chanin 1980). Assuming an upper level temperature the density profile is integrated downward.

The error in derived temperature depends, both on the error in density measurements and in the assumed model pressure (in present study, from CIRA 86 model) at the top. The error due to the uncertainty in the assumed model pressure value at the top altitude disappears very fast and after 10 to 15 km it is less than 1% (Hauchcorne & Chanin 1980; Ferrare et al., 1995).

PRL Rayleigh Lidar System

The PRL Rayleigh lidar set up at Mt Abu is shown in Fig. 1. It consists of a pulsed Nd-YAG laser with second harmonic generator, a 90-cm diameter Cassegrain telescope (secondary mirror of 25 cm diameter and effective focal length of 737 cm) which, receives the back-scattered signal, a thermoelectric cooled Photo Multiplier Tube (PMT) that operates in photon counting mode, a signal processing unit and a data processor. The specifications of the system are provided in Table 1. The laser beam is transmitted vertically upwards with the help of a 45° incidence, 2-inch diameter ultra hard dielectrically coated high-energy laser mirror. The optical axis of the telescope was initially kept at a distance of about 0.5 m from the transmitter optics but moved away to about 2m in November 2000. The field of view of the telescope (about 1 m Rad) is kept large in comparison to the laser beam divergence so as to accommodate the beam totally above a threshold altitude which is about 2 km in the present set up. An interference filter having a maximum transmission of about 20 % at 532 nm and a bandwidth of 1 nm is used to reduce the background noise. A PMT, which is cooled below -25° C using a thermoelectric cooler, is used to detect photons. By

gating the PMT, high intensity signals from low altitudes are avoided which could cause saturation of the detector and also may produce the signal-induced noise (SIN). The PMT is turned on for 0.5 ms, which corresponds to a range of 75 km. A programmable delay generator is used to control switching ON/OFF the PMT gain. The delay can be varied from 1 ms to 999 ms in steps of 1 ms. For the Rayleigh scattering mode of operation a delay of 150 ms is introduced so as to collect data from 22.5 km to 97.5 km. A 1024 channel SR-430 data processor is used for data handling and online display. A vertical bin size of 96 m corresponding to 0.64 ms is used for Rayleigh scattering mode. Normally 6000 laser shots (in 10 minutes) are integrated for each file of data stored.

Observations and Data Analysis

The Lidar is operated in Rayleigh mode for about 5 nights in each month around new Moon except during the monsoon season. Photon counts integrated for 10 minutes were stored in each data file. Initially the

lidar was operated for an hour for density measurements but since April 2001 this was increased to 2 hours. The total number of nights of operation in different months during which good quality data are obtained is given in Table 2. Data are available for more than 10 nights for most of the months, 7 nights in May and 3 nights each in June and September. No measurements could be made during the months of July and August due to cloudy sky condition.

The schematic for the off-line data processing is shown as flowchart in Fig. 2. It involves dead time correction (Evans 1955) to the photon count values and adding the photon counts of 5 range bins to give effective range bins of 480 m each. All the photon count profiles of 10 minutes duration each are integrated. A 5 point linear running mean is applied to further smooth the photon count profile. The background noise is removed at this stage, by estimating the average photon counts between 85 and 95 km, which is subtracted from each bin. Range correction is then applied and the density values are obtained from the range corrected photon count profile.

Table 1. Specifications of the PRL Rayleigh Lidar System

Laser Type Average Power Energy per pulse Pulse Repetition rate Beam divergence	Nd:YAG (581C-10, Quantel, France) 4.4 W at 532 nm 440 mJ at 532 nm 10 Hz 0.6 mrad
Receiver Antenna Telescope type Diameter (Primary mirror) Diameter (Secondary mirror) Field of view Power-aperture product	Cassegrain :effective focal length 737 cm 90 cm 25 cm 1 mrad 2.6 Wm ²
Optics Interference filter Central wavelength Filter bandwidth Transmission Photomultiplier Mode of operation Dark counts	532 nm 1 nm 20 % 9813A (Electron Tubes, UK) Photon counting mode ~ 300 counts/sec at 20° C
Signal Processor Type Bin width	SR430, Stanford Research Systems, USA (100 MHz) 640 ns (96 m) with no inter channel dead time

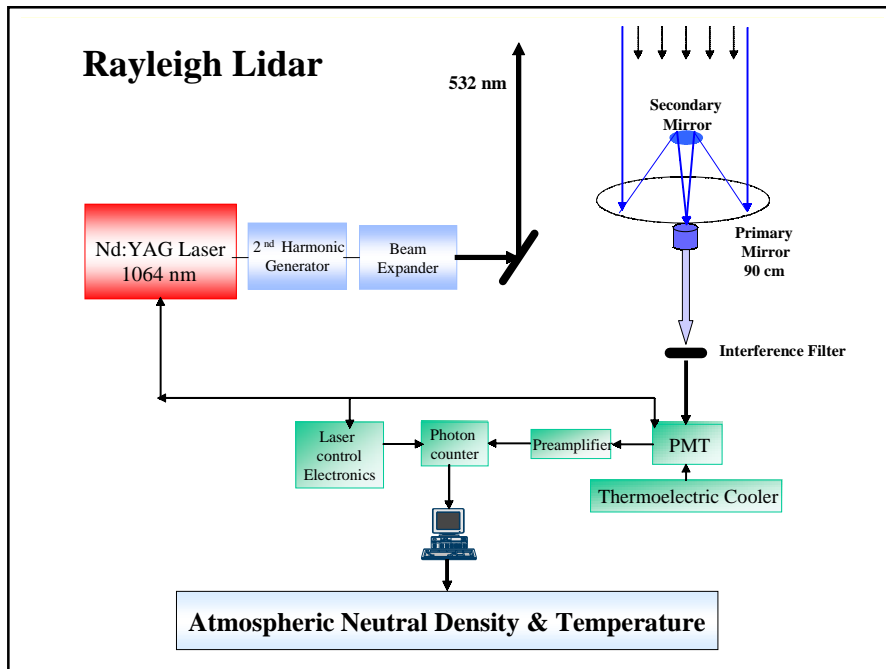


Figure 1. Block diagram of the PRL Rayleigh lidar set up at Guru Shikhar, Mt Abu.

Table 2. Rayleigh Lidar Observations at Mt. Abu, India (November 1997 to November 2001)

Month Year	Jan	Feb	Mar	Apr	May	Jun	Jul	Aug	Sep	Oct	Nov	Dec	Total Nights
1997											1	5	6
1998	3	2	3	C	C	CL	CL	CL	CL	1	3	3	15
1999	3	3	3	4	CL	CL	CL	CL	C	C	C	C	13
2000	C	4	5	8	3	3	CL	CL	CL	CL	6	6	35
2001	4	2	7	5	4	CL	CL	CL	3	8	7		40
Total	10	11	18	17	7	3	CL	CL	3	9	17	14	109

C -Instrument not working
 CL -Clouds

The pressure value from COSPAR International Reference Atmosphere-86 (CIRA-86) model (Fleming et al. 1990) is fitted at 80 km to derive the temperature profile. The uncertainty in model pressure at top of the profile is about 10-15 %. Its contribution to derived temperature decreases rapidly and less than 2% at about 15 km from the top. Finally the measurement error in temperature (1s level) is computed.

An example of the range-corrected signal, which is directly related to density, is shown in Fig. 3a up to an altitude of 80 km. The temperature profile is derived from the relative density profile following the

method described in section 2 with pressure value from CIRA-86 model, fitted at 80 km. The derived temperature profile plotted up to 75 km is shown in Fig. 3b along with the error (one sigma level). The temperature values obtained from CIRA-86 model are also shown for comparison.

A study was made on the error in derived temperature as a function of data length and range width. The data sequence of 4 hour was made during the night of October 21, 2001. Temperature profiles were obtained from this data set using different data lengths corresponding to 10, 30, 60, 90, 120, 180 and 240 minutes. Fig. 4 shows the variation of the error

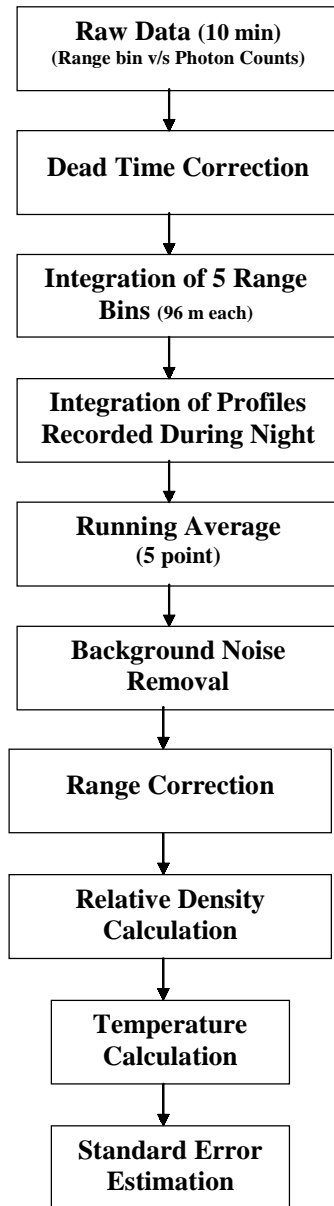


Figure 2 Flow chart of processing the lidar data for temperature derivation.

with altitude for different data lengths. The error for 10 minutes of data length varies from 1 K at 40 km to more than 30 K at 70 km. For 30 minutes these vary from about 0.5 K at 40 km to 20 K at 70 km. The errors vary from less than 0.5 K at 40 km to 15 K at 70 km for 60 minutes of data length and from less than 0.5 K at 40 km and 11 K at 70 km for 120 minutes of data length. Data length of an hour was used for measurements initially and 120 minutes later on that give temperature values with errors (one sigma level) of 2.1 (1.4) K at 50 km, 5(3.5) K at 60 km and 15.4 (10.5) K at 70 km.

RESULTS

Day to day variability

To study the day to day variability temperature profiles on available nights have been studied for three selected months of January, May and October 2001. Fig. 5a shows temperature profiles on four nights of 22-25 January 2001. The geophysical variability (described by the standard deviation of the measured values) and the standard error in measurement (one sigma level) are also plotted in the side panel as a function of altitude. The temperature values are relatively higher on 23 January than other days. The variability varies from 2 K to 10 K with lowest around 45-55 km. Temperature profiles for four nights during the month of May 2001 are shown in Fig. 5b. Signatures of gravity waves are clearly noticed on each of the four nights. The standard deviation is within 2-5 K below 65 km and about 10 K above 65 km. However in view of the error being more than the standard deviation, above 65 km this may not be considered significant. In Fig. 5c temperature profiles are shown for the nights 16, 17, 19-22 October 2001. The integration time of 120 minutes is used on most of the nights. The standard deviation again varies between 2 K and 10 K with lowest values in the region of 40-50 km.

Below 60 km the standard error in measurements are less than the standard deviation whereas above 70 km the error in measurements is greater than the standard deviation. The altitude variation of the standard deviation for January 2001 shows high values around 40 km (7 K) and 70 km (10 K) with a minimum around 51-52 km (1K). The standard deviation during May 2001 shows fluctuations between 3 and 5 K up to 65 km and a peak at 68 km (10 K). The altitude variation of the standard deviation for the month of October shows peaks around 37 km (4 K), 52 km (5 K) and 69 km (8 K) with low values of 1- 2 K between 41 and 49 km.

Year to Year variability

To examine the year to year variability, mean monthly temperature profiles have been estimated for different years. Fig. 6a shows the mean monthly profiles for the month of March during the years 1998 to 2001. The standard error in measurement and the standard deviation are also shown in the side panel. The standard deviation is least (4 K) around 40-42 km and values close to 5 K at altitudes below 53 km. The standard deviation values show a peak of 14 K between 60 and 67 km. Higher values are seen above 70 km

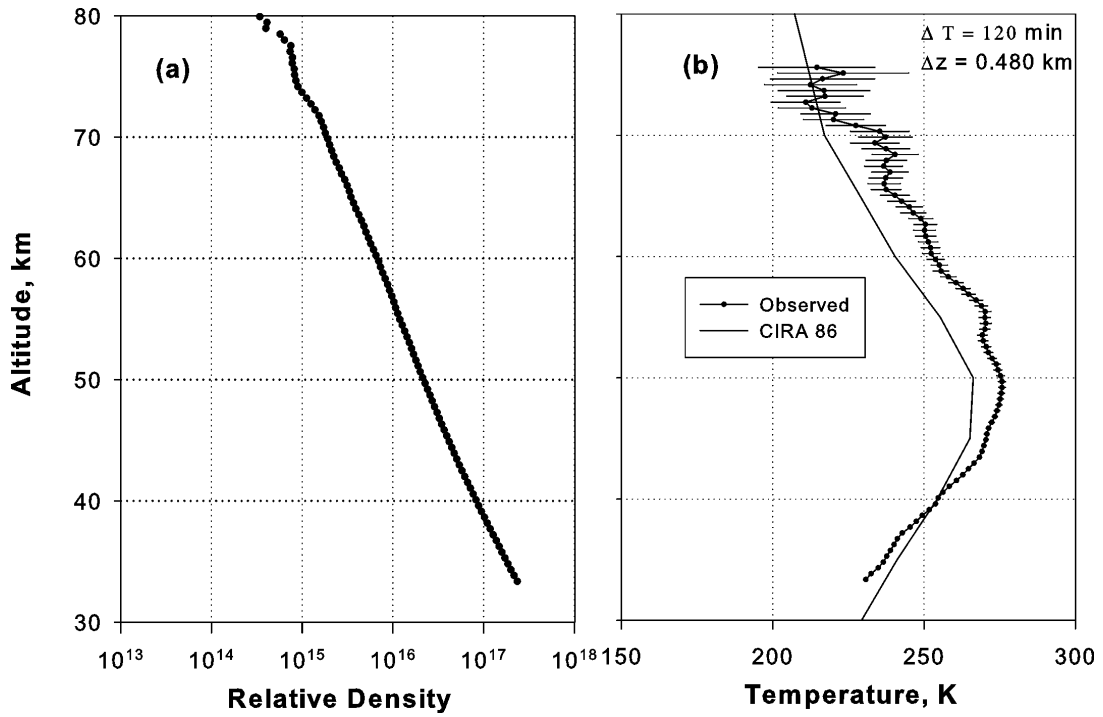


Figure 3(a) Relative density profile from 33 to 80 km obtained from the range corrected photon count profile and (b) temperature profile from 33 to 75 km along with the error in measurement (one sigma level). CIRA-86 temperature profile is also shown.

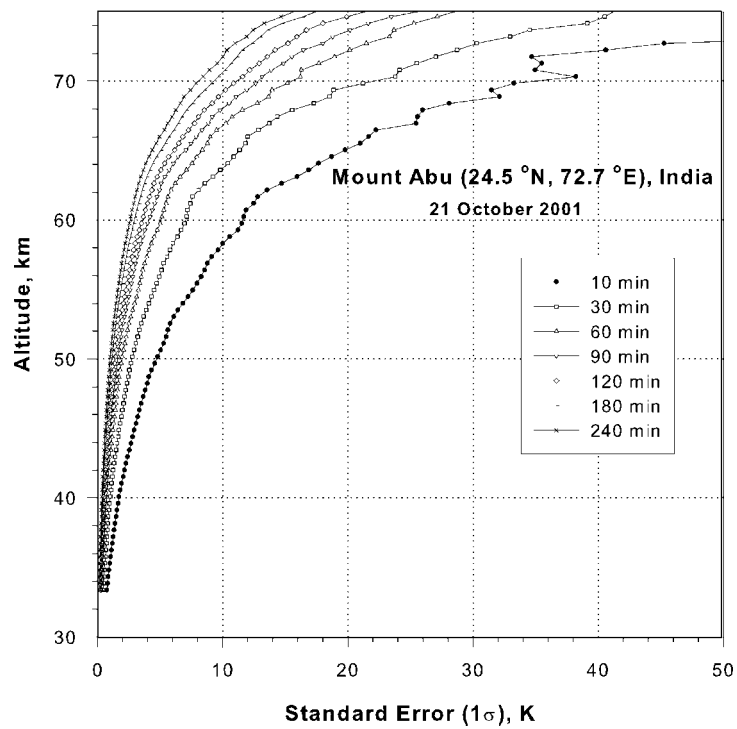


Figure 4 Variations of the error in derived temperature from density measurements with altitude for different integration time.

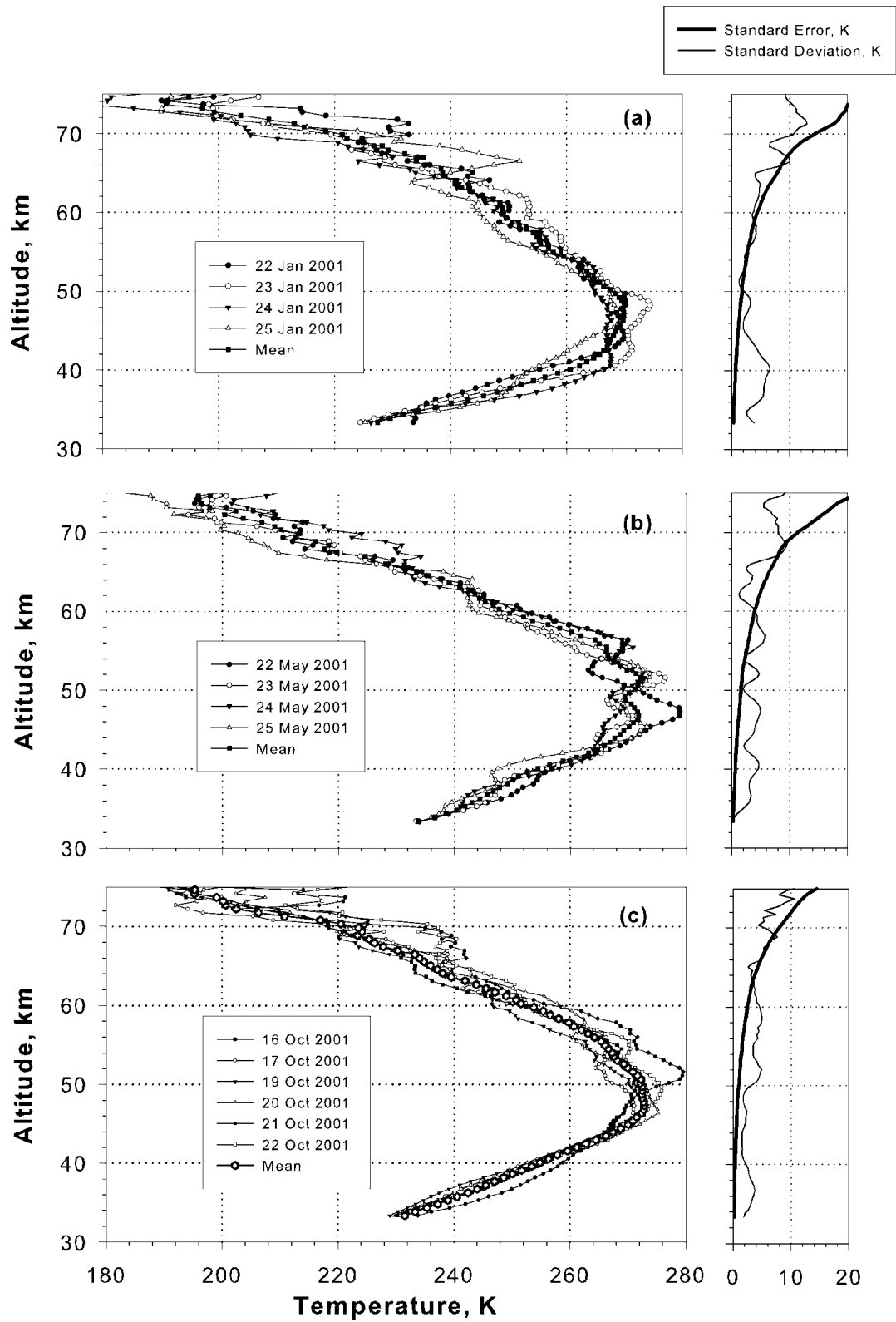


Figure 5. Temperature profiles along with the mean profile for (a) four successive nights of 22 to 25 January 2001, (b) four successive nights of 22 to 25 May 2001 and (c) six successive nights of 16 to 22 October 2001. The standard deviation and the standard error in measurement (one sigma level) are also shown in the side panels.

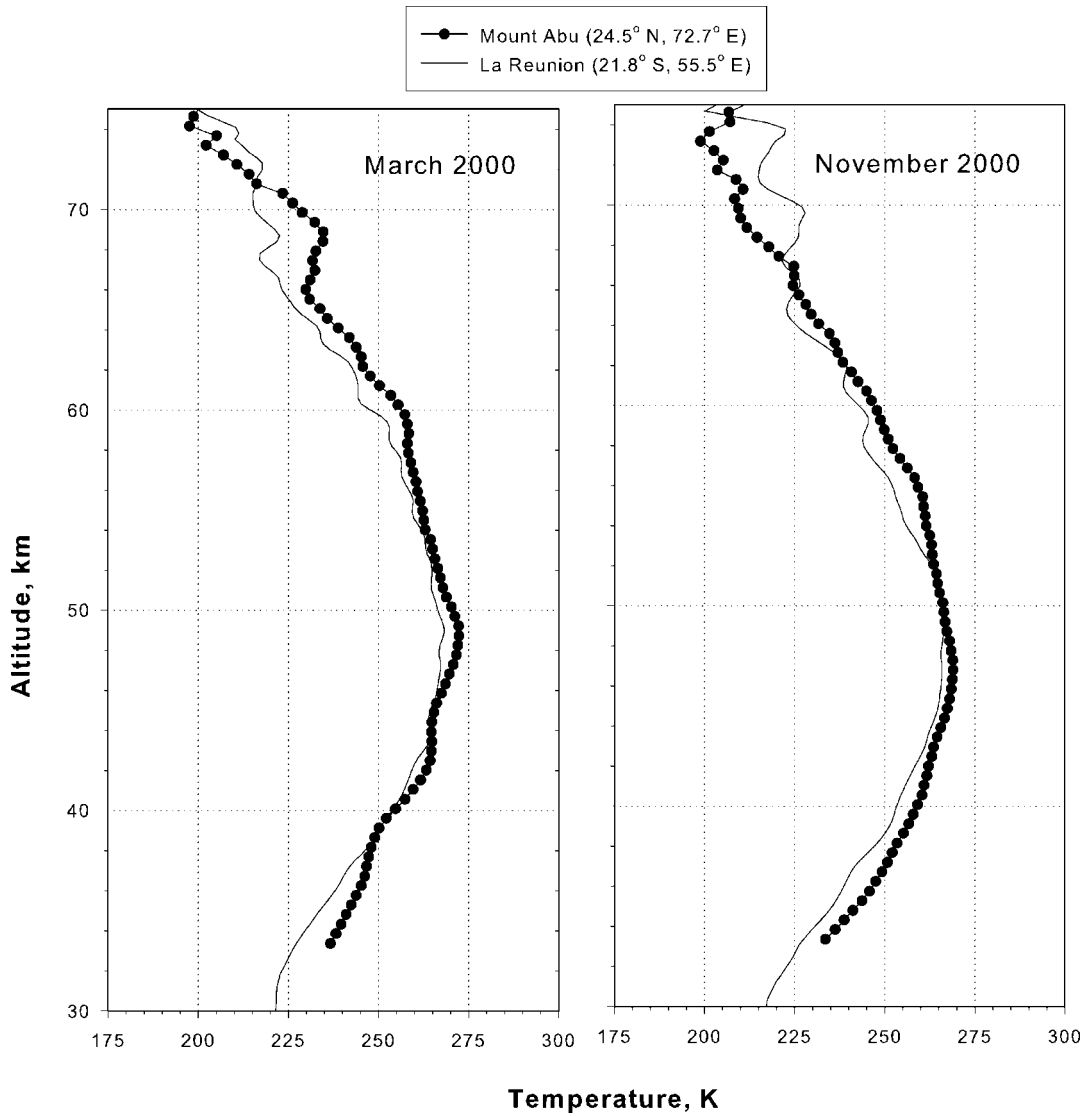


Figure 6. Monthly mean temperature profiles and the average profile for (a) March 1998 to 2001 and (b) November 1997 to 1998 and 2000 to 2001. The standard deviation and the standard error in measurement (one sigma level) are also shown in the side panels.

but the error are larger there. Similar plots for the month of November for the years 1997 to 2001 are shown in Fig. 6b. Year to year variability is also more prominent above 50 km. The variability is least around 40-50 km with a value of 5 K. Standard deviation values are 15 K at 35 km and 62 km. The standard error exceeds standard deviation values above 70 km. Thus the results of Figs 5 and 6 clearly indicate a trend of lower variability around the region 40-50 km.

Mean temperature profiles

Mean temperature profiles have been computed from the available temperature profiles over Mt. Abu. These

are compared with the CIRA-86 model profiles for the location of 25° N. The mean monthly temperature profiles based on the entire data are shown in Fig.7 for the months September to May. The horizontal bars indicate the standard error in the mean. The number of points are less during the months of June and September (3 each) while no measurements were possible during July and August due to the monsoon season. The observed temperature values are in agreement with CIRA-86 model values between 30 to 65 km during the months of December, January and February. For other months values match below 50 km but are up to 10-15 K higher than the CIRA-86 model values at altitudes of 50-70 km. The differences

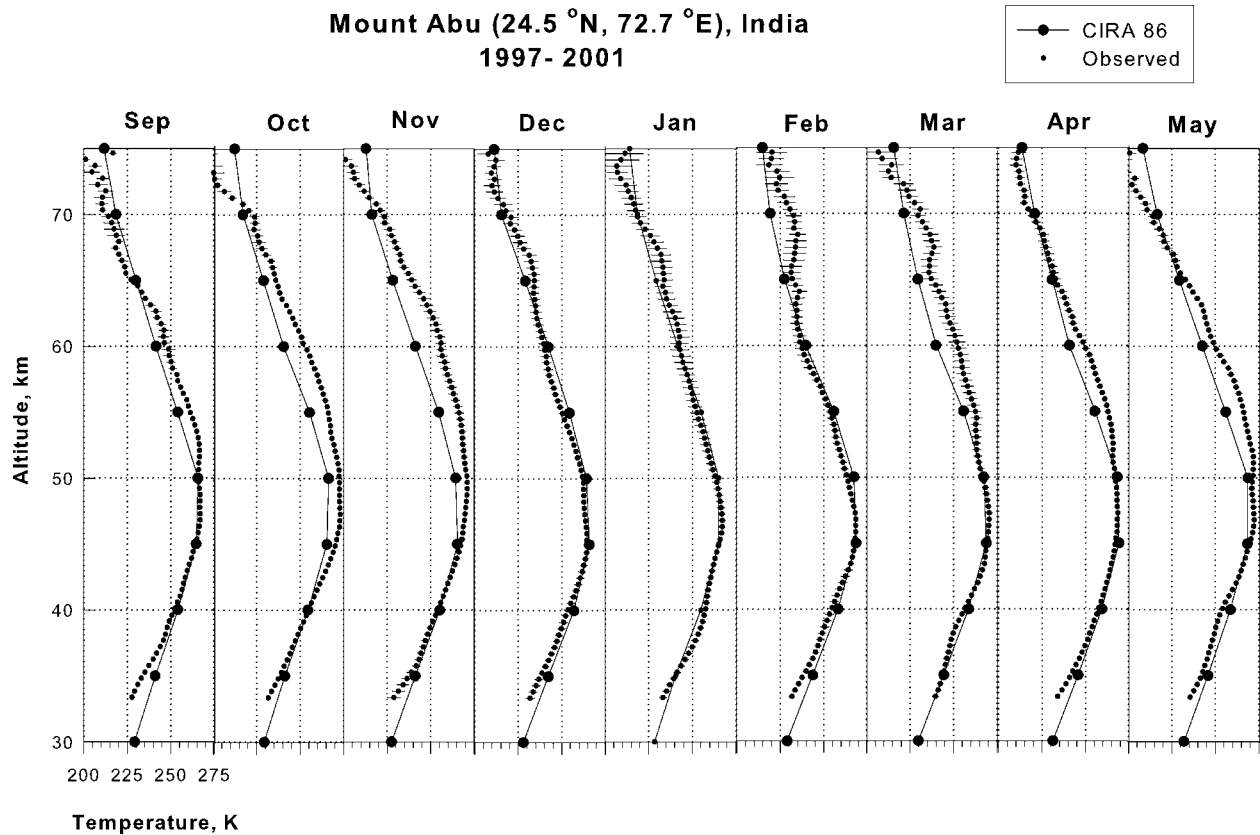


Figure 7. Monthly mean temperature profiles for each month (September to May) averaged over the period November 1997 to November 2001 along with the CIRA-86 profiles.

are largest during equinoxes. Small but significant deviations are also seen below 35 km for almost all of the months shown here. Similar deviations were also seen in the mean temperature profiles from Gadanki reported by Siva Kumar, Rao & Krishnaiah (2003).

Contour map of the temperature structure plotted in the grid of months versus altitude is shown in Fig. 8a with a resolution of 2 K. For comparison similar contour map based on the CIRA-86 model is also shown in Fig 8b. There does not seem to be significant change in the temperature value with months below about 45 km in either the observed or model values. Observed stratopause values are slightly higher than the CIRA-86 values and are highest for the equinoctial months of October and March-May as described by model also. Between 50 and 65 km comparatively larger change with season is seen in the observed values with equinoctial maxima. Above 70 km the model shows winter maximum and summer minimum. The observed values indicate the trend for higher values for January-February.

The contours of the difference between the observed temperature and the CIRA-86 values are shown in Fig. 9. Below 50 km the difference is less than 5 K. The difference is high around 60 km with values about 15 K during October–November and 10 K during March. Another peak of more than 10 K is noticed during May. The differences are again high above 70 km during equinoctial months. However the errors too are large in this altitude region.

Stratopause Variability

To study the stratopause variations in detail the stratopause temperature and altitude level are derived from each of the temperature profile. The mass plot of the stratopause height and the stratopause temperature are shown in Fig. 10. There is an indication of an annual variation in both the stratopause temperature and height showing lowest values during winter months indicating a trend of maximum during local summer months. However more observations in summer (June) are needed to

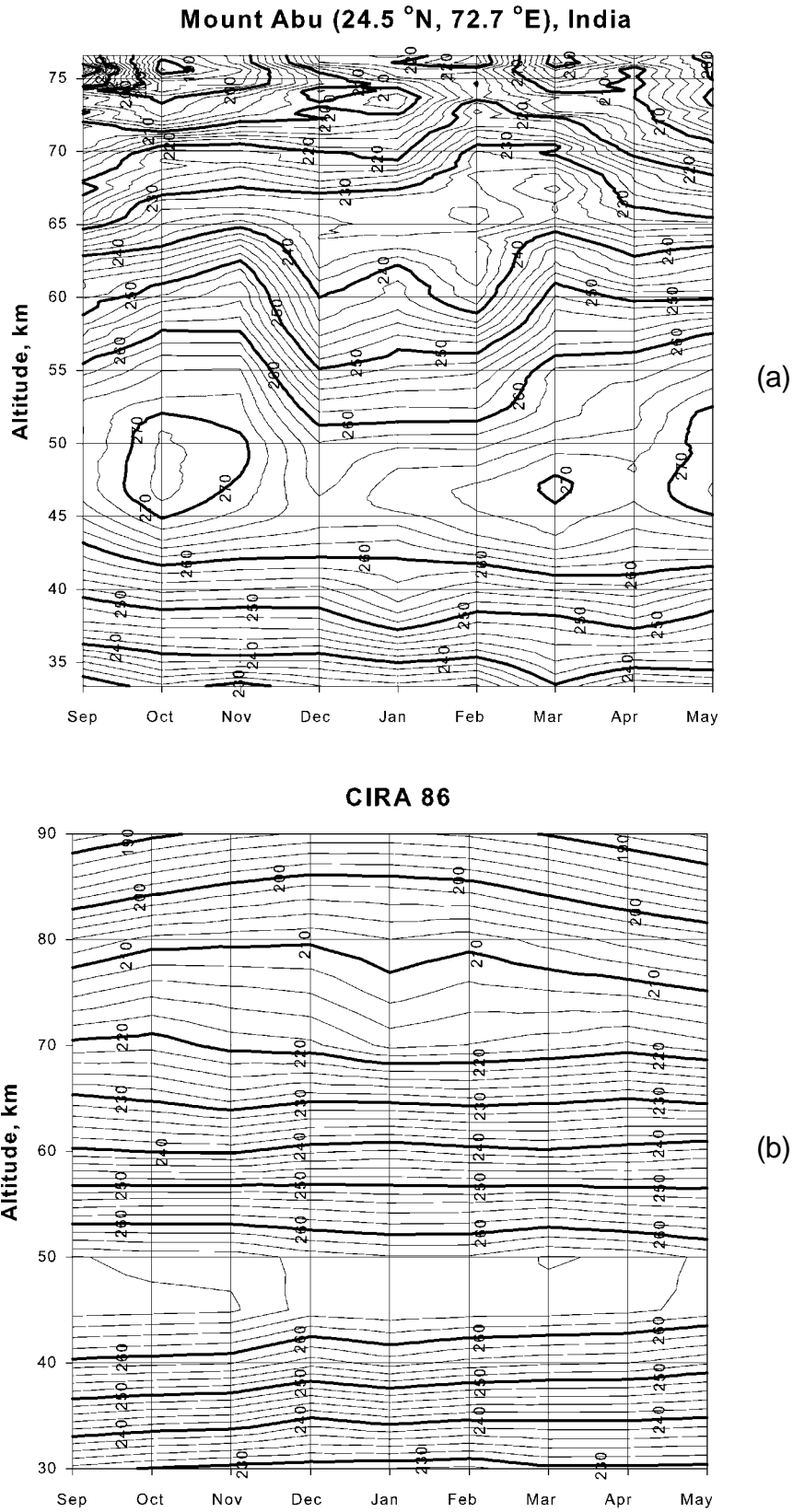


Figure 8. Contour maps of temperature plotted in the grid of altitude versus months for (a) Observed over Mt. Abu and (b) CIRA-86.

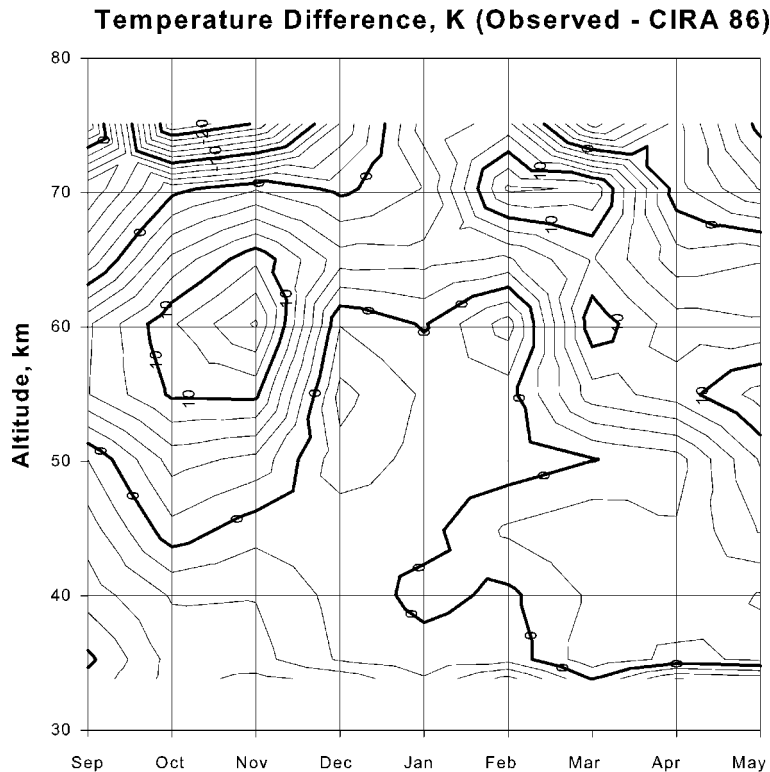


Figure 9. Contour maps of the difference in observed temperature from CIRA-86 values plotted in the grid of altitude versus months

confirm it. There is a day to day variability and for any month the difference between minimum and maximum values is about 15 K in temperature and about 5 km in the altitude of stratopause. The histograms of the occurrence of the stratopause temperature are shown in Fig 11a. The temperature varies between 254 and 290 K with 95% of values between 258 and 282 K. The mean value of the stratopause temperature is 271 K with standard deviation of 5.7 K. The histograms of the occurrence of the stratopause height are shown in Fig 11b. The stratopause height varies between 44 and 52 km with a mean value of 48 km and standard deviation of 1.7 km.

Comparison with other observations

Using the radiosonde measurements at Madras (13.1° N, 78.4° E), Port Blair (11.7° N, 92.7° E), Minicoy (8.3° N, 73.2° E) and Trivandrum (8.5° N, 76.9° E) and the M-100 weekly rocket flights from Thumba (Trivandrum) for the period 1971-76, a reference atmosphere model for low latitudes over the Indian region was made by Sasi & Sengupta (1979). In the region of upper stratosphere equinoctial maxima occur

in temperature while in the mesosphere (70-80 km) a maximum occurs in winter with equinoctial minima. The variability in temperature was less than 5 K (one sigma level) below 60 km and about 10 K above 68 km. The variability was lowest around 50-55 km. Based on the measurements from balloons at Trivandrum and M-100 rocket launchings from Thumba over 16 years, a reference atmosphere has been constructed for the equatorial region in India (Sasi 1994). The stratopause was located at 47 km with a temperature of 264 K. A comparison with CIRA-86 model shows that the reference temperatures are cooler than the CIRA-86 temperatures above 40-45 km. Seasonally the temperature in the upper stratosphere shows equinoctial maxima and above 70 km a winter maximum. Seasonal variation in the stratosphere is mainly produced by ozone heating by solar ultraviolet flux. Seasonal dependence in the breaking of gravity waves and tides in the upper mesosphere may be source for large seasonal variation in temperature above 70 km.

A comparison of the annual mean and seasonal mean temperature profiles over Mt. Abu with the CIRA-86 and the equatorial model of Sasi & Sengupta (1979) is shown in Fig. 12. The three seasons of winter

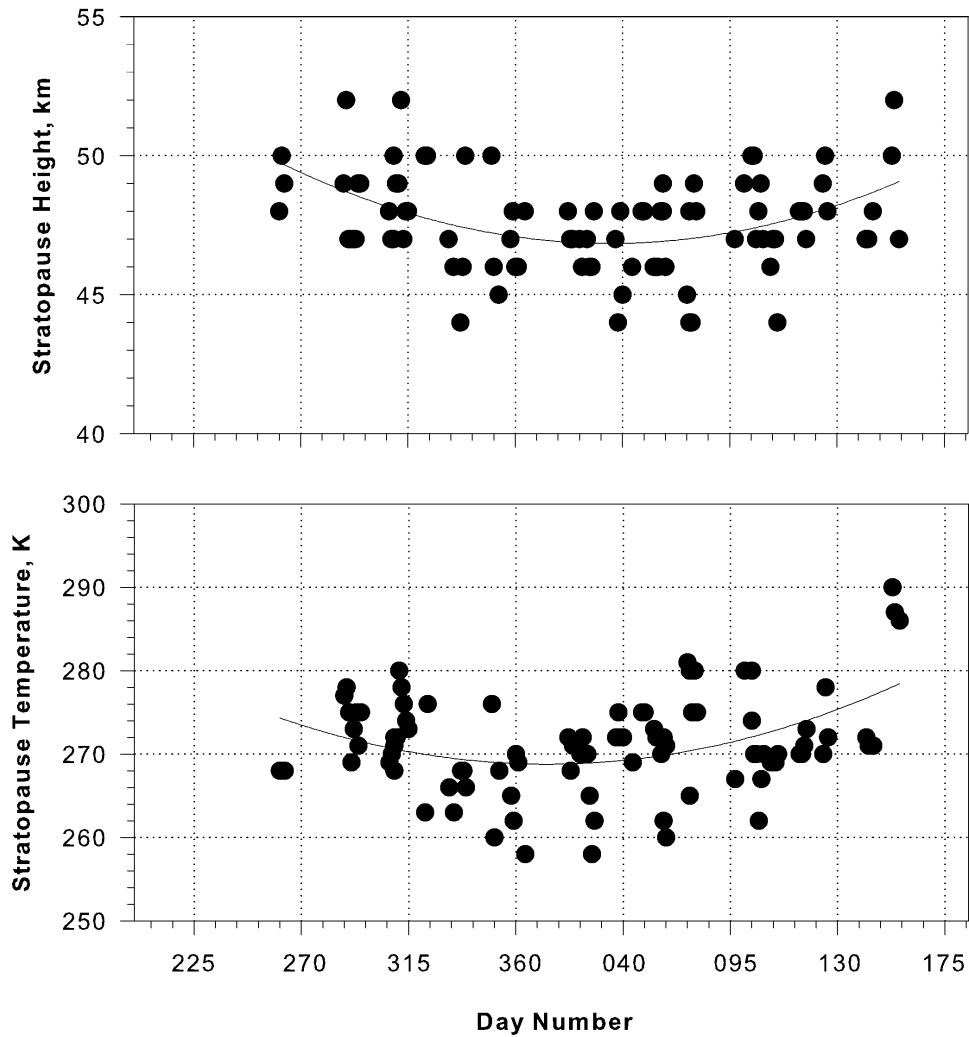


Figure 10. Plots of day to day values of (a) stratopause height and (b) stratopause temperature over Mt. Abu.

(November to February), equinoxes (March/April and September/October) and summer (May, June) are used in the comparison. Up to stratopause the observed values at Mt. Abu are lower than the equatorial model by a few Kelvin. Above 50 km however, the observed values over Mt. Abu are higher than the equatorial model by up to 15 K. Below 50 km the observed annual mean values are in close agreement with CIRA-86. The observed values are higher by up to 7 K between 50 and 70 km. Examination of the observed profiles for different seasons shows very close agreement below 60 km during winter but the observed values are more than the model values by up to 7 K between 60 and 70 km. During equinoxes and summer close agreement is seen below 50 km and observed values are higher by up to 10 K between 50 and 70 km.

A comparison of the observed temperature at Mt. Abu with satellite measurements (HALOE) is shown in Fig. 13. HALOE satellite details, observations and related middle atmospheric temperature studies can be found in papers (Russell et al. 1993; Hervig et al. 1996; Remsberg et al. 2002b). The measurements are for the night of 8 March, 1999. The temperature values for CIRA-86 and the MSISE-90 (Mass Spectrometer Incoherent Scatter Extended -90; Hedin 1991) are also shown. While the values for the two models are fairly close to each other there are differences with the Rayleigh lidar and satellite measurements. Between 50 and 70 km both the lidar and satellite derived values are higher than the two models. Below 50 km while the satellite values are in close agreement with models the lidar values show wave like perturbations.

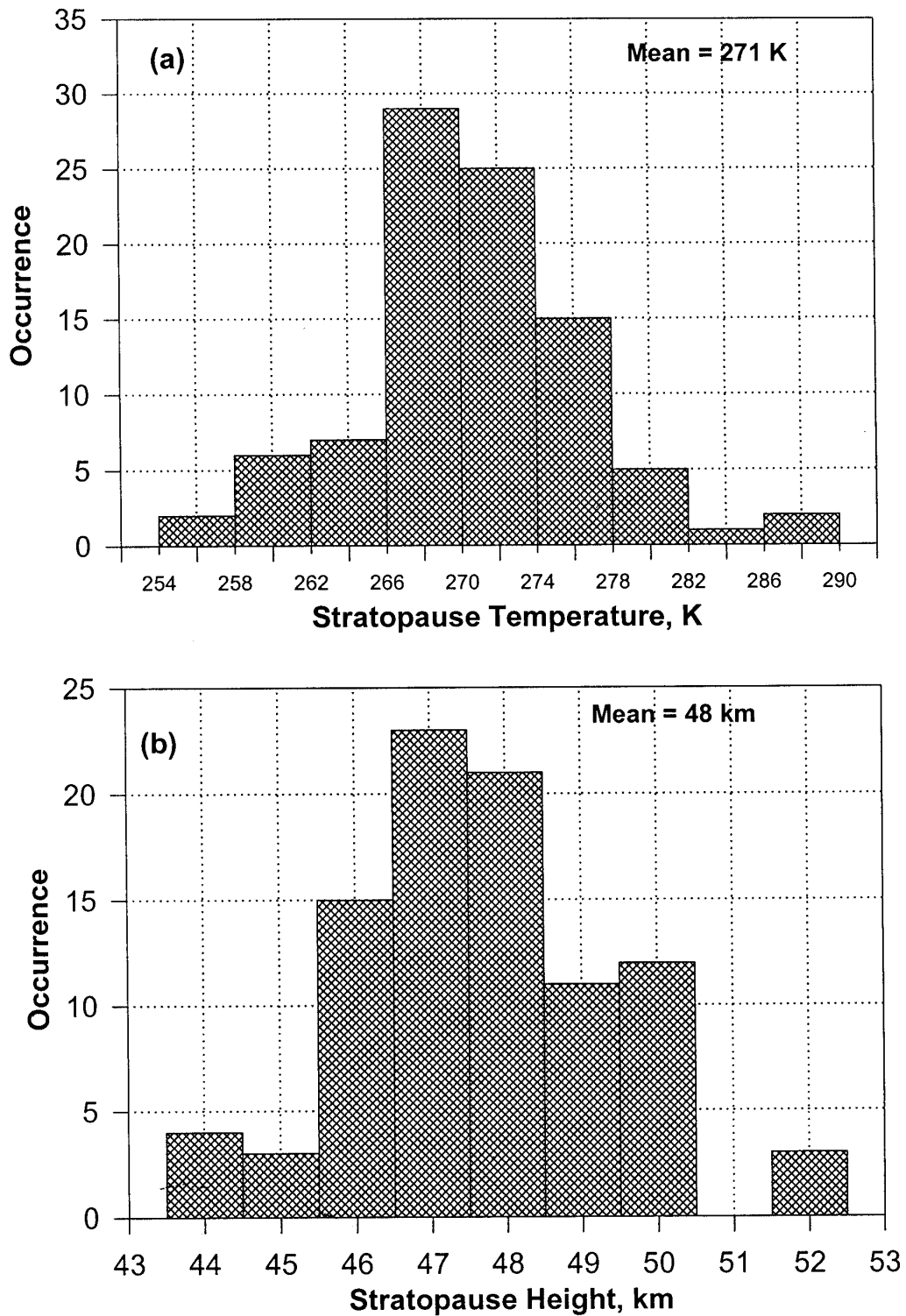


Figure 11. Histograms of occurrence of (a) stratopause height and (b) stratopause temperature over Mt. Abu.

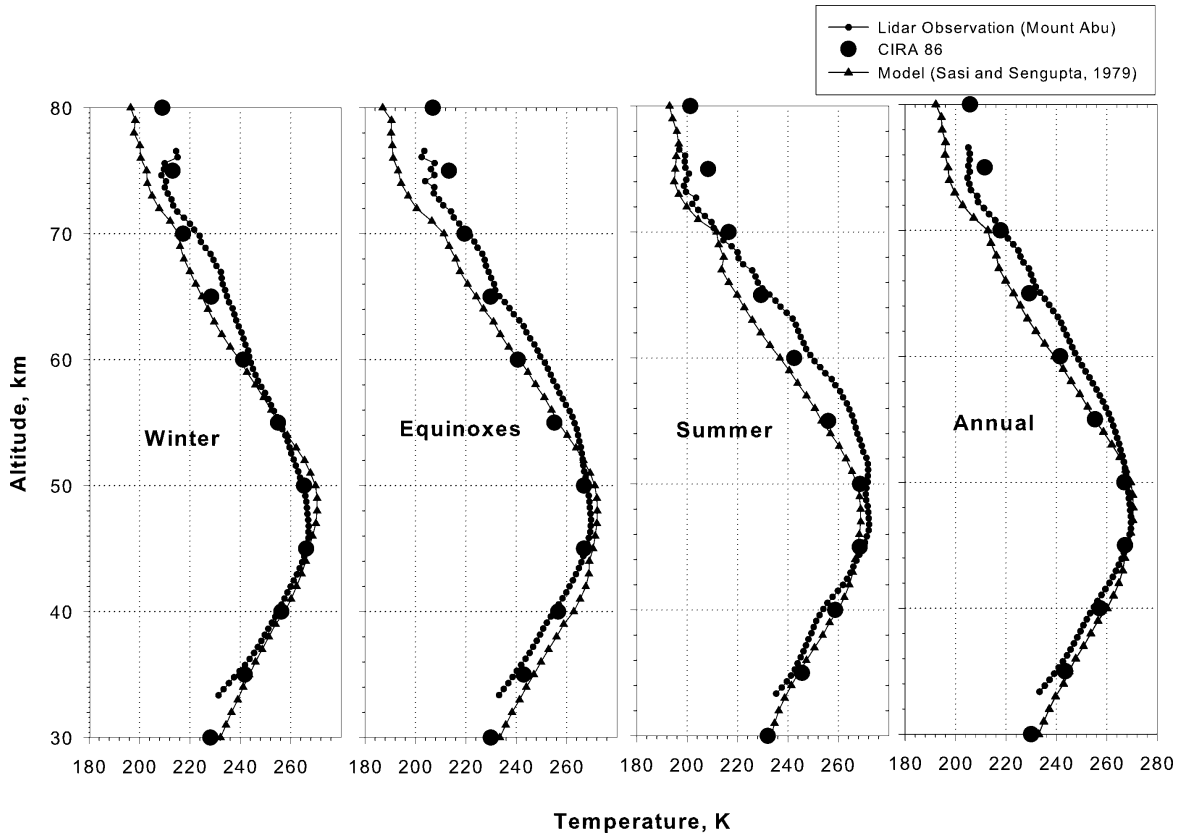


Figure 12. Altitude profiles of the annual mean and seasonal mean temperature obtained from (a) lidar observations at Mt. Abu, (b) CIRA-86 model and (c) equatorial model of Sasi and Sengupta (1979).

A Nd-YAG laser based lidar (at NMRF, India in collaboration with CRL, Japan) is operational at Gadanki (13.5° N, 79.2° E), a low -latitude station in India. Some of the early measurements from Gadanki made during January 1999 are reported by Parameswaran et al. (2000). Kumar et al. (2001) have reported temperature profiles for different months based on 119 nights of data during the period March 1998- February 2000. The mean temperature profile for January 1999 (based on 8 nights of data) was compared with CIRA-86 model. CIRA-86 temperatures were higher than the lidar derived values right from 35 km onwards. The difference was about 10 K between 50 and 70 km. The measurements at Mt. Abu however are higher than the CIRA-86 temperature above 50 km. Siva Kumar, Rao & Krishnaiah (2003) have recently reported climatology of temperature structure over Gadanki based on 240 nights of observations from March 1998 to July 2001. Two distinct equinoctial maxima in temperature were seen in the stratopause level. The stratopause level ranged between 43 and 58 km with maximum frequency of occurrence in the height range of 47-48

km with a standard deviation of 3.2 km. The stratopause temperature ranged between 248 and 279 km with maximum frequency of occurrence in the temperature range of 261-262 K with standard deviation of 4.4 K. Thus while the stratopause level at Gadanki and Mt. Abu are at same level the stratopause temperature is about 10 K cooler at Gadanki than at Mt. Abu. The variabilities in stratopause temperature and level are of similar order at the two locations. Compared to CIRA-86 model the observed temperature values in the height range of 70-80 km differed by up to 10 K. The variabilities in temperature were found to be less than 6 K for altitudes below 70 km with lowest values of less than 2 K below 60 km. The standard deviation ranged between 6 and 16 K for the altitude region of 70-80 km with highest values during equinoxes.

We have compared the temperature structure for the Mt. Abu and Gadanki sites for the night of 24 April 2001 as shown in Fig. 14a. The temperature values at the two locations are within 3-4 K of each other up to 60 km but higher at Mt. Abu up to 15 K at higher altitudes. Though the Mt. Abu values are

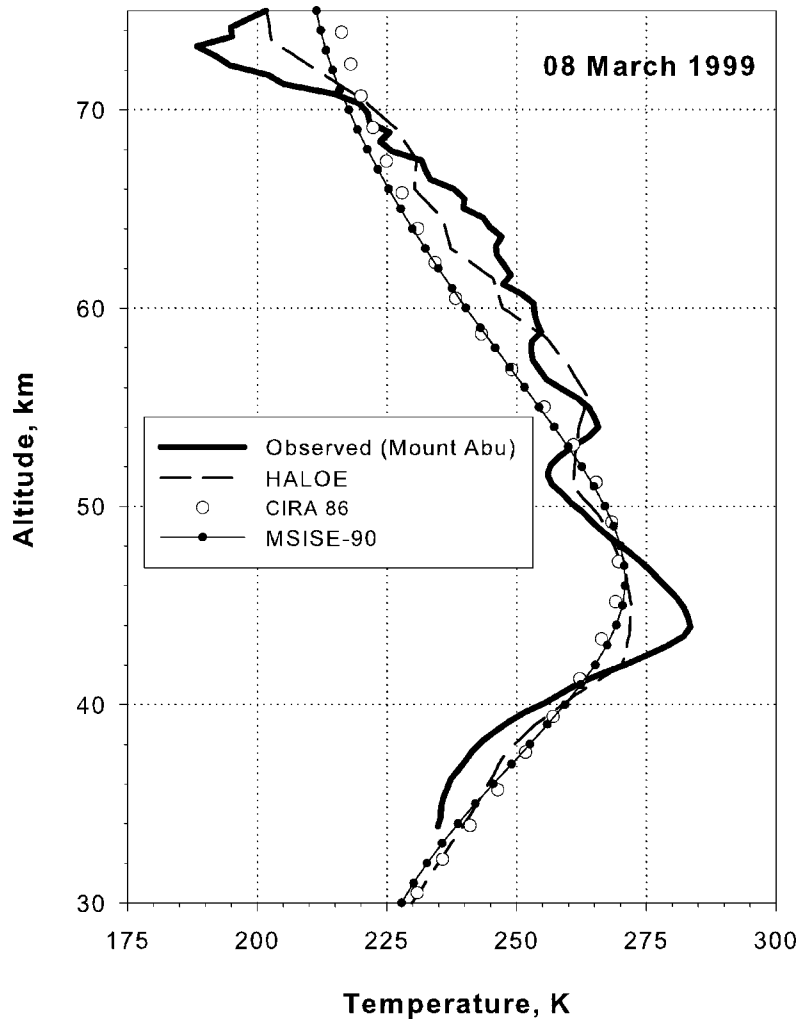


Figure 13. Temperature profile over Mt. Abu for the night of March 8, 1999 compared with the profile obtained from satellite (HALOE) and from the models, CIRA-86 and MSISE-90.

slightly higher than Gadanki values the trend is similar. The mean monthly temperature profiles for January and April averaged over the entire period are also compared with similar profiles for Gadanki in Fig. 14b. The profiles for Gadanki are reproduced from the work reported by Siva Kumar et al. (2003). For the month of January temperature values are higher for Mt. Abu by up to 12 K except in the altitude region of 50-60 km where Gadanki values are higher by few degrees. For the month of April the values at Mt. Abu are higher throughout the altitude region the difference ranging up to 15 K above 65 km. Some of the difference in the temperature values at Mt. Abu and Gadanki could be due to the latitudinal variation in the temperature at these two locations.

Rayleigh lidar observations are available at tropical latitudes in other longitude regions also (Nee et al.

1995; Nambhoorthi et al. 1999). Dao et al. (1995) made measurements at Air Force Maui Optical Site, Haleakala (20.7° N, 203.7° E) during the year 1993. Rayleigh/Raman and Na Wind/Temperature lidars provided temperature values from 25 to 103 km. Rayleigh and vibrational Raman techniques have been operational at Mauna Loa (19.5° N, 155.6° W) to retrieve temperature in the altitude range between 15 and 90 km (McDermid et al. 1995; Leblanc et al. 1998). A comparison of the mean temperature profiles over Mt. Abu and Mauna Loa for the month of March 2000 is shown in Fig. 15. The data for 3 nights (9-11 March for Mt. Abu and 8, 10 and 14 March for Mauna Loa) are used in this comparison. The values for Mt. Abu are slightly higher, the difference being larger above 50 km. Another noticeable difference is in the presence of mesospheric inversion around 68 km seen

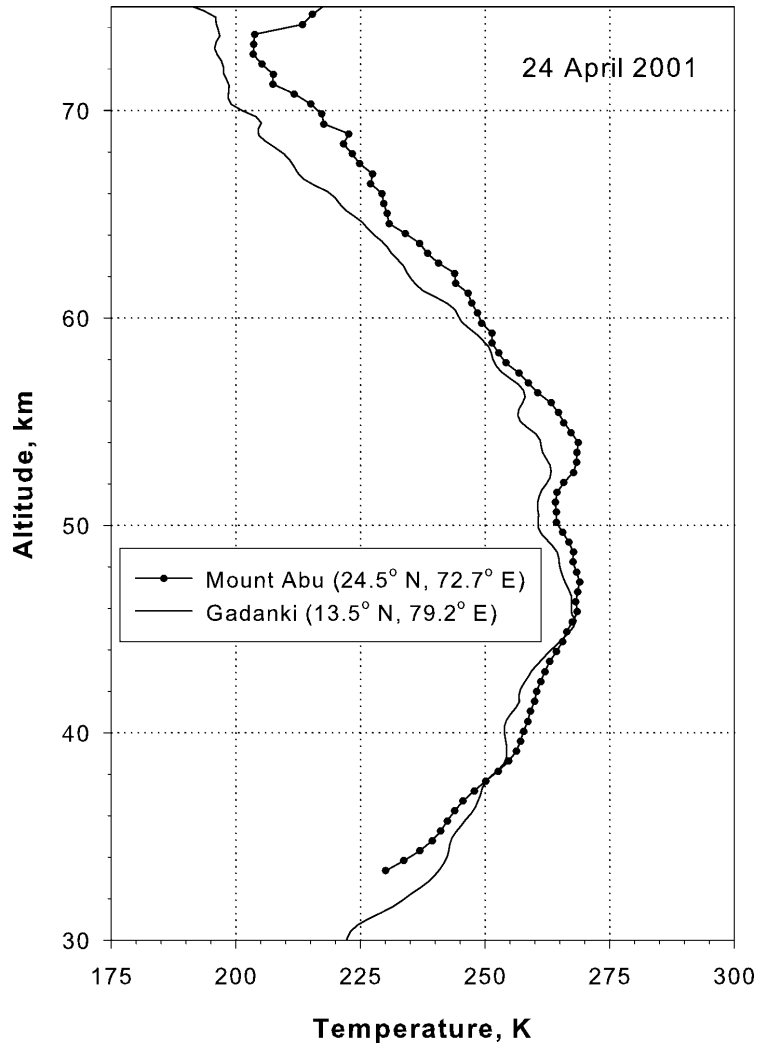


Figure 14a. Temperature profile over Mt. Abu and at a low latitude station Gadanki for the night of April 24, 2001.

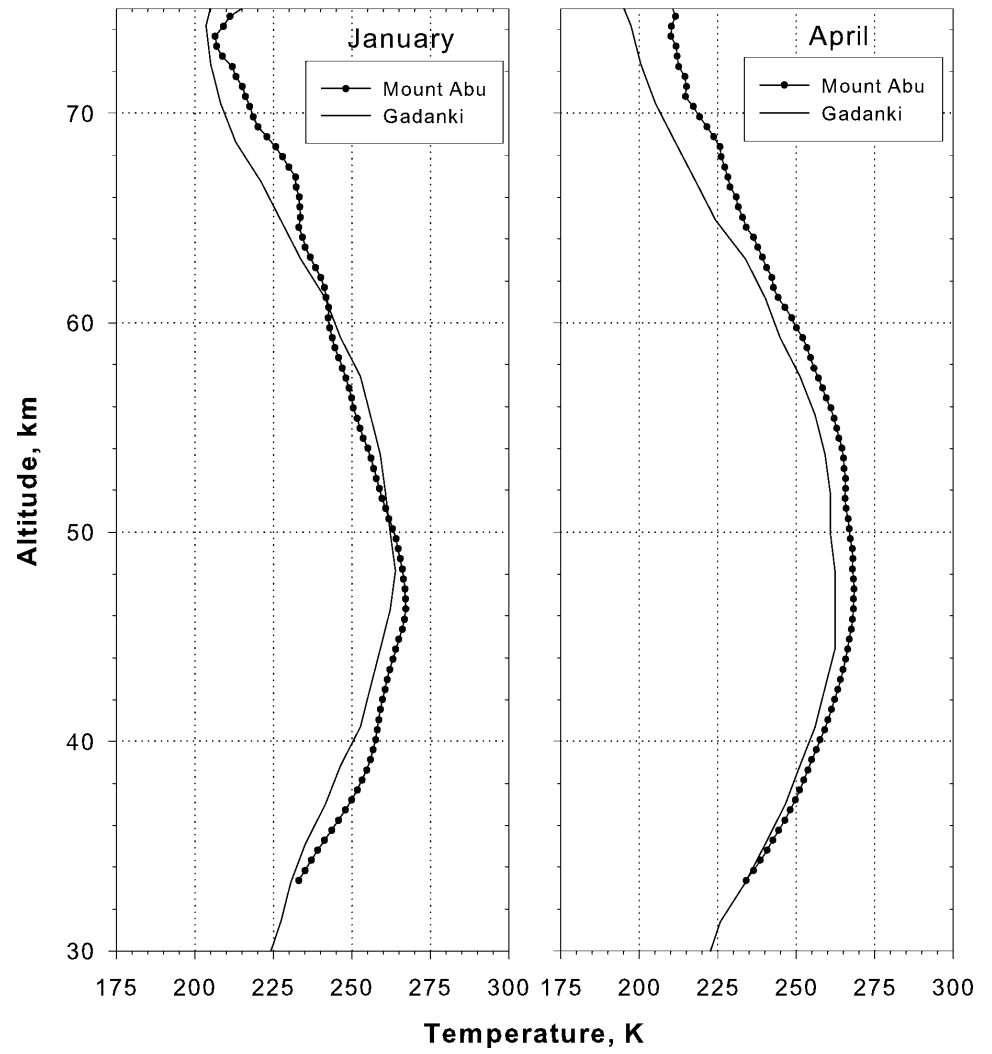


Figure 14b. Mean temperature profiles over Mt. Abu and Gadanki for the months of January and April.

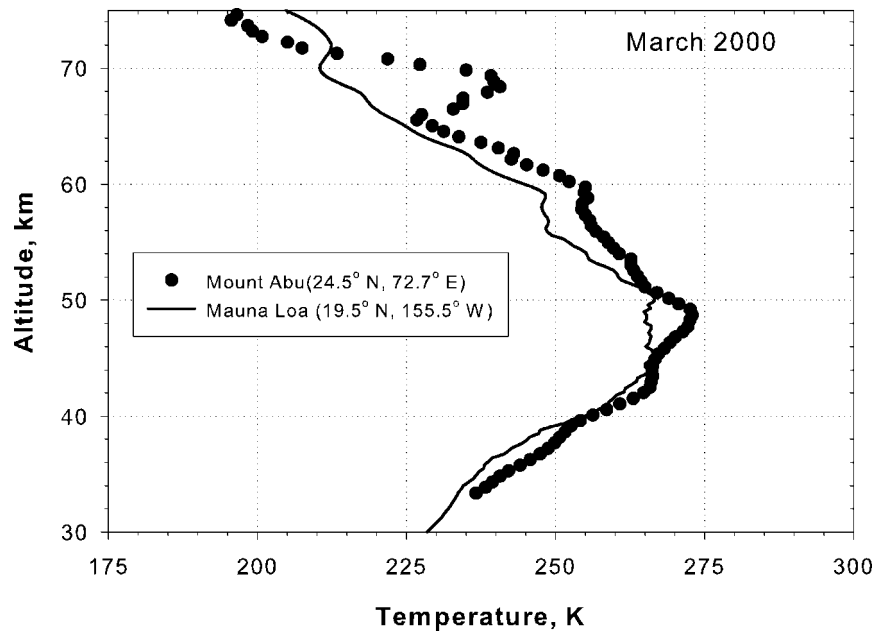


Figure 15. Mean temperature profiles over Mt. Abu and another tropical station Mauna Loa for March 10, 2000.

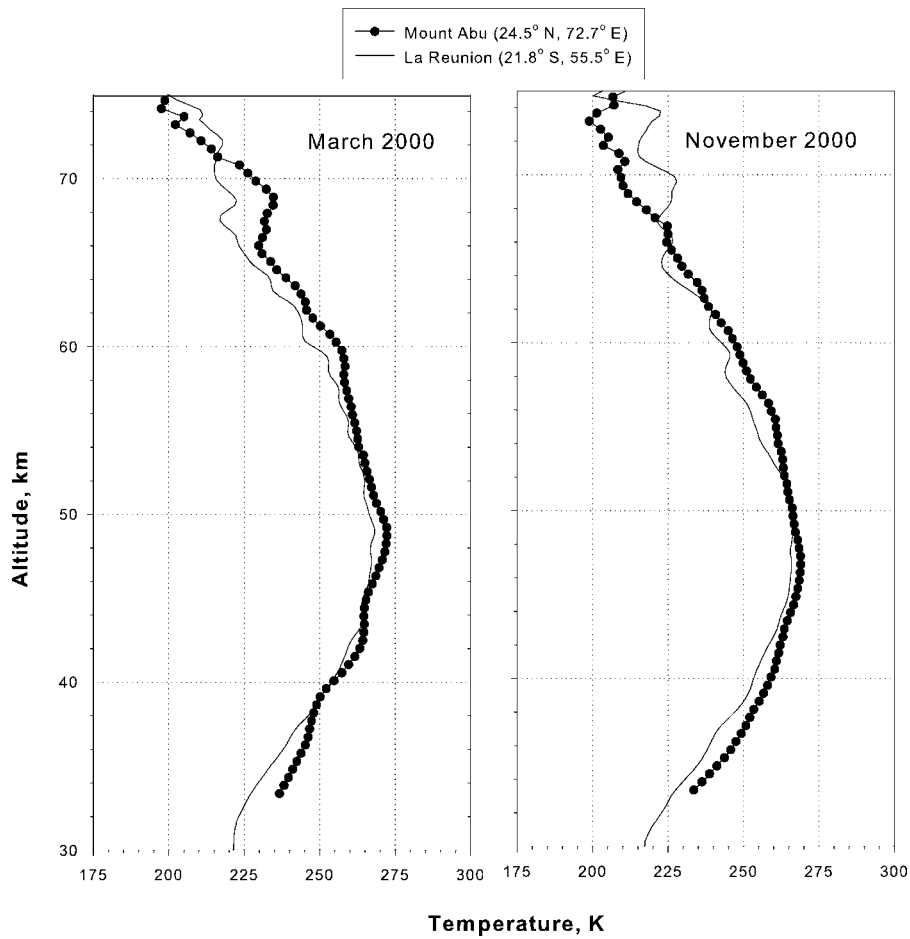


Figure 16. Monthly mean temperature profiles over Mt. Abu and another tropical station La Reunion for the months of March and November of the year 2000.

at Mt. Abu. Beyond 72 km the values at Mauna Loa are slightly higher than at Mt. Abu.

The temperature profiles over Mt. Abu are also compared with another tropical station La Reunion (21.8° S, 55.5° E). Monthly mean temperature profiles for the months of March 2000 and November 2000 over the two locations are shown in Fig. 16. The profiles are in fairly good agreement except for the region of about 66-70 km for the month of March 2000. Temperature values observed at Mt. Abu are higher than the values at La Reunion by about 15 K but for the region 65-70 km La Reunion values are higher than the Mt Abu values by similar amount. Thus considering the errors in measurements the temperature values at Mt. Abu are close to the values at other tropical stations of similar latitudes.

SUMMARY

Based on 4 years of Rayleigh lidar measurements from Mt. Abu, a tropical latitude station in India, climatology of the temperature structure between 33-70 km is obtained and compared with the CIRA-86 model, MSISE-90 and Indian low latitude model by Sasi and Sen Gupta (1979). The observed temperatures are in close agreement with CIRA-86 model below 50 km but are higher by up to 10 K between 50-70 km. The observed values over Mt. Abu are lower than the equatorial model values at Trivandrum by a few degrees below stratopause but higher by up to 15 K above 50 km. The day to day variability (standard deviation) is less than 5 K below 50 km and up to 15 K above 50 km. The year to year variability is less than 10 K below 50 km and up to 20 K above 50 km. The variability is least around 40-42 km. The stratopause level varies between 44 and 52 km with a mean value of 48 km. The stratopause temperature varies between 260 and 280 K with a mean value of 271 K. Both the stratopause height and temperature are lowest during winter months. The seasonal variation shows equinoctial maxima with an indication of a maximum in summer also but more observations are needed to ascertain this.

ACKNOWLEDGEMENTS

The authors would like to thank Prof. B H Subbaraya for the encouragement and Prof. L Thomas for helpful discussions. The authors would also like to thank Prof. R K Varma and Prof. G S Agarwal, the past and present Directors of PRL for their constant encouragement and support to the lidar program. Thanks are also due to Shri J T Vinchhi for help in lidar operation at Mt. Abu. The lidar project is

financed by the Dept. of space, Govt. of India through their funds to the Physical Research Laboratory.

Authors are thankful to the Upper Atmosphere Research Satellite (UARS) Project, (Code 916), and the Distributed Active Archive Center (Code 902), Greenbelt, MD 20771 for providing HALOE satellite data through the website <http://haloedata.larc.nasa.gov/Haloe>. The data for Mauna Loa used in this publication was obtained as part of the network for the detection of stratospheric change (NDSC) and is publicly available (<http://www.ndsc.ncep.noaa.gov>). Thanks are also due to Denis Faduilve, Laboratoire de Physique de la Atmosphere, La Reunion University for the data of Reunion.

REFERENCES

- Browell E. V., 1989. Differential absorption lidar sensing of ozone, Proc. IEEE, 77, 419-432, 1989.
- Chanin M. L. & Hauchecorne, A., 1981. Lidar observation of gravity and tidal waves in the stratosphere and mesosphere, J. Geophys. Res., 86, 9715-9721.
- Chanin M. L. & Hauchecorne, A., 1984. Lidar studies of temperature and density using Rayleigh scattering, in 'Handbook for MAP', ed. by R. A. Vincent, 13, 87-99.
- Chanin M. L. & Hauchecorne, A., 1996. Lidar study of temperature and dynamics of the middle atmosphere, Ind. J. Radio & Space Phys., 20, 1-11.
- Clemesha B. R., 1984. in 'Handbook for MAP', Vol. 13, ed. by R. A. Vincent.
- Dao P. D., R. Farley, R., Tao, X. & Gardner, C.S., 1995. Lidar observations of the temperature profile between 25 and 103 km: evidence of strong tidal perturbation, Geophys. Res. Lett., 22, 2825- 2828.
- Evans R. D., 1955. PP 7, in "The Atomic Nucleus", McGraw-Hill Book Company.
- Ferrare R. A., McGee, T.J., Whiteman, D., Burris, J., Owens, M., Butler, J., Barnes, R.A., Schmidlin, F., Komhyr, W., Wang, P.H., McCormick, M.P. & Moller, A.J., 1995. Lidar measurements of stratospheric temperature during STOIC, J. Geophys. Res., 100, 9303-9312.
- Fleming, E. L., Chandra, S., Barnett, J.J. & Corney, M., 1990. Zonal mean temperature, pressure, zonal wind and geopotential height as function of latitude, Adv. Space Res., 10, 11-59.
- Gardner C. S., 1989. Sodium resonance fluorescence lidar applications in atmospheric science and astronomy, Proc. I E E E, 77, 408-418.

- Gobbi G. P., Souprayen, C., Congeduti, F., Donfrancesco, G.Di., Adriani, A., Viterbini, M. & Centurioni, S., 1995. Lidar observations of middle atmosphere temperature variability, *Ann. Geophysicae*, 13, 648-655.
- Hauchecorne A. & Chanin, M.L., 1980. Density and temperature profiles obtained by lidar between 35 and 70 km, *Geophys. Res. Lett.*, 7, 565-568.
- Hedin A. E., 1991. Extension of the MSIS thermosphere model into the middle and lower atmosphere, *J Geophys. Res.*, 96, 1159-1172.
- Hervig M. E., Russell, J.M., Gordley, L.L., Drayson, K., Stone, R.E., Thompson, M.E., Gelman, I.S., McDermid, A., Hauchecorne, A., Keckhut, P., McGee, T.J., Sinh, U.N. & Gross, M.R., 1996. A Validation of temperature measurements from the Halogen Occultation Experiment, *J Geophys. Res.*, 101, 10277-10286, 1996
- Hinkley E. D., 1976. ed. "Laser monitoring of the atmosphere", Springer-Verlag, Berlin, Heidelberg, New York, p 1-380.
- Jayaraman A., Acharya, Y.B., Subbaraya, B.H. & Chandra, H., 1995a. Nd:YAG backscatter lidar at Ahmedabad (23° N, 72.5° E) for tropical middle atmospheric studies. *Appl. Optics*, 34, 6937.
- Jayaraman A., Ramchandran, S., Acharya, Y.B. & Subbaraya, B.H., 1995b. Pinatubo volcanic aerosol layer observed at Ahmedabad (23°N), India, using neodymium: yttrium /aluminium/ garnet backscatter lidar, *J. Geophys. Res.*, 100, 23209-23214.
- Jayaraman A., Acharya, Y.B., Chandra, H., Subbaraya, B.H., Ramchandran, S. & Ramaswamy, S., 1996. Laser radar study of the middle atmosphere over Ahmedabad, *Ind. J. Radio & Space Phys.*, 25, 318-327.
- Jenkins D. B., Wareing, D.P., Thomas, L. & Vaughan, G., 1987. Upper stratospheric and mesospheric temperatures derived from lidar observations at Aberystwyth, *J. Atmos. Terr. Phys.*, 49, 287-298, 1987.
- Kent, G. S. & Wright, R.W.H., 1970. A review of laser radar measurements of atmospheric properties, *J. Atmos. Terr. Phys.*, 32, 917-943.
- Kumar V. S., Kumar, Y.B., Raghunath, K., Krishnaiah, M., Mizutani, K., Aoki, T., Yasui, M., & Itabe, T., 2001. Lidar measurements of mesospheric temperature inversion at a low latitude, *Ann. Geophysicae*, 19, 1039-1044.
- Leblanc T., McDermid, I.S., Keckhut, P., Hauchecorne, A., She, C.Y., & Krueger, D.A., 1998. Temperature climatology of the middle atmosphere from long-term measurements at middle and low latitudes, *J Geophys. Res.*, 103, 17191-17204.
- McDermid I. S., Walsh, T.D., Deslis, A. & White, M., 1995. Optical systems design for a stratospheric lidar system, *Appl. Opt.*, 34, 6201-6210.
- Measures, R. M., 1984. *Laser remote sensing: Fundamentals and Applications*, 510 pp., John Wiley, New York.
- Menzies R. T. & Hardesty, R.M., 1989. Coherent Doppler lidar for measurements of wind fields, *Proc. IEEE*, 77, 449-462.
- Namboothiri S. P., Sugimoto, N., Nakanei, H., Matsui, I. & Murayama, Y., 1999. Rayleigh lidar observations of temperature over Tsumuba: Winter thermal structure and comparison studies, *Earth Planets Space*, 51, 825-832.
- Nee J. B., Wang, G.B., Lee, P.C. & Lin, S.B., 1995. Lidar studies of particles and temperature of the atmosphere: First results from National Central University lidar, *Radio Science*, 30, 4, 1167-1175.
- Parameswaran K., Sasi, M.N., Geetha Ramkumar, Prabha R. Nair, Deepa, V., Krishnamurthy, B.V., Nayar, S.R.P., Revathy, K., Mrudula, G., Satheesan, K., Bhavanikumar, Y., Sivakumar, V., Raghunath, K., Rajendraprasad, T. & Krishanaiah, M., 2000. Altitude profiles of temperature from 4 to 80 km over the tropics from MST radar and lidar, *J. Atmos. Sol. Terrest. Phys.*, 62, 1327-1337.
- Reagan J. A., McCormick, M.P. & Spinhirne, J.D., 1989. Lidar sensing of aerosols and clouds in the troposphere and stratosphere, *IEEE*, 77, 433-448.
- Remsberg E., Bhatt, P., Deaver, P. & Lance, E., 2002b. Seasonal and Long-term variations in the middle atmosphere temperature from HALOE on UARS, *J Geophys. Res.*, 107, 10.1029/2001JD001366.
- Russell J. M. III., Gordley, L.L., Park, J.H., Drayson, S.R., Hesketh, W.D., Cierone, R.J., Tuck, A.F., Frederick, J. E., Harries, J.E. & Crutzen, P.J., 1993. The Halogen Occultation Experiment, *J Geophys. Res.*, 98, 10777-10797.
- Sasi M. N., 1994. A reference atmosphere for the Indian equatorial zone, *Ind. J. Radio & Space Phys.*, 23, 299-312.
- Sasi M. N. & Sengupta, K., 1979. A model equatorial atmosphere over the Indian zone from 0 to 80 km, Scientific report ISRO-VSSC-SR-19.
- Siva Kumar V., Rao, P.B. & Krishnaiah, M., 2003. Lidar measurements of stratosphere-mesosphere thermal structure over a low latitude : Comparison with satellite data and models, *J. Geophys. Res.*, 108(D11), 4342, doi:10.1029/2002JD003029.
- Shibata T., Kobuchi, M. & Maeda, M., 1986a. Measurements of density and temperature profiles in the middle atmosphere with a XeF

lidar, Appl. Opt., 25, 685-688.

Shibata T., Fukuda,T. & Maeda, M., 1986b. Density fluctuations in the middle atmosphere over Fukuoka observed by XeF Rayleigh lidar, Geophys. Res. Lett., 13, 1121-1124.

Thomas L.,1987. Laser radar observations of middle-atmosphere structure and composition, Phil. Trans. Roy. Soc., A323, 597-609.

Thomas L., Marsh,A.K.P., Wareing,D.P., Astin,I. &

Chandra, H.,1996. VHF echoes from the midlatitude mesosphere and thermal structure observed by lidar, J. Geophys. Res., 101, 12867-12877.

Whiteway J. A. & Carswell,A.I., 1994. Rayleigh lidar observations of thermal structure and gravity wave activity in the high Arctic during a stratospheric warming, J Atmos. Sci., 51, 3122-3136.

(Accepted 2005 June 13. In original form 2005 February 25)



PROF.HARISH CHANDRA

Born and educated in Uttaranchal obtained M.S. (Physics) degree from Agra University in 1964. Joined Physical Research Laboratory, Ahmedabad as research scholar in 1964 and after completing Ph.D degree in ionospheric physics in 1970 as faculty. Has worked in India and abroad on a number of ground based radio and optical techniques and rocket-borne in-situ experiments to study earth's atmosphere and ionosphere. Has published more than 200 research papers.



MR.SOM KUMAR SHARMA

Mr.Som Kumar Sharma is currently working as a Scientist-SD at the Space & Atmospheric Sciences Division of the Physical Research Laboratory, Ahmedabad and his field of specialization is earth's ionosphere and LIDAR based studies of the earth's middle atmosphere.



DR.Y.B.ACHARYA

Dr.Y.B.Acharya is currently working as an Engineer-SG at the Space & Atmospheric Sciences Division of the Physical Research Laboratory, Ahmedabad and his field of specialization is space-borne instrumentation (rocket and balloon) for the study of atmospheric parameters and also variety of ground based instrumentation such as LIDAR etc. He is also involved in the PRL's High Energy X-ray payload for Chandrayaan-I (India's Moon Mission).



DR.A.JAYARAMAN

Dr.A.Jayaraman is currently a Professor at the Space and Atmospheric Sciences Division of the Physical Research Laboratory, Ahmedabad and his field specializations are aerosols, lidar and atmospheric radiative transfer.